

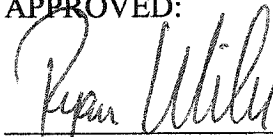
PREVIEW

**DIRECT INJECTION SPARK IGNITION FUEL SPRAY
CHARACTERIZATION UNDER SIMULATED INJECTION
STRATEGIES**

ROBERT EDMOND HENNESSEY, JR.

Department of Mechanical and Industrial Engineering

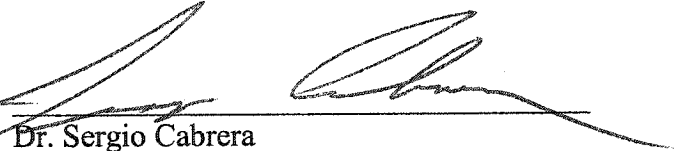
APPROVED:



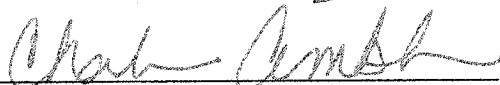
Dr. Ryan Wicker, Chair



Dr. Ahsan Choudhuri



Dr. Sergio Cabrera



Associate Vice President
for Graduate Studies

This Thesis Is Dedicated to my Mom and Dad

PREVIEW

PREVIEW

**DIRECT INJECTION SPARK IGNITION FUEL SPRAY
CHARACTERIZATION UNDER SIMULATED INJECTION
STRATEGIES**

by

ROBERT EDMOND HENNESSEY, JR., B.S.M.E.

THESIS

**Presented to the Faculty of the Graduate School of
The University of Texas at El Paso
in Partial Fulfillment
of the Requirements
for the Degree of**

MASTER OF SCIENCE

Department of Mechanical and Industrial Engineering

THE UNIVERSITY OF TEXAS AT EL PASO

July 2001

UMI Number: ep05529

PREVIEW

UMI[®]

UMI Microform ep05529

Copyright 2003 by ProQuest information and Learning Company.

All rights reserved. This microform edition is protected against
unauthorized copying under Title 17, United States Code.

ProQuest Information and Learning Company
300 North Zeeb Road
P.O. Box 1346
Ann Arbor, MI 48106-1346

Acknowledgments

I would like to thank Dr. Ryan Wicker, director of the NASA Flow and Thermal Imaging Laboratory, for presenting me the opportunity to perform this research and for the guidance he provided throughout my graduate studies. I would also like to thank my other committee members, Dr. Ahsan Choudhuri and Dr. Sergio Cabrera for their assistance and feedback during the writing of this thesis. Dr. Rolando Quintana deserves a great deal of credit for providing the statistical analysis presented in this work. I would also like to thank NASA for donating NASA-FAR grant NAG4-150, which funded a great portion of this work.

Several other people in the department deserve recognition. I would like to thank Oscar Acosta, Rudy Aguilar, Carlos Herrera, and Carrie McKillip for their assistance in the acquisition and construction of several laboratory components. My co-workers in the NASA FTIL, Aaron Hutchison and Hugo Loya have assisted me greatly in the completion of this work. Other student researchers that have contributed in one way or another throughout my graduate studies include Jose Bustamante, Jorge Camacho, Juvenal Herrera, Fernando Jasso, Frank Medina, Miguel Perez, and Luis Terrazas. I would also like to thank three of my lifelong, best friends, James Perkins, Rudy Pino, and Nathaniel Smith, for their support and friendship.

Finally, I would like to thank my Mom and Dad for all their love and support that they have given me throughout my life. My parents were always there for me when I needed them most. My Mom and Dad gave up everything so I could chase my dreams, and for that I can never repay them.

This thesis was submitted to the supervising committee on July 10, 2001.

Executive Summary

The work contained here characterizes the instantaneous fuel spray structure of a dense, transient spray under non-motored, simulated injection strategies. These strategies utilize the variation and control of in-cylinder pressure to simulate in-cylinder density at the time of injection in the motored case, and temperature of the fuel as well as that of a simulated piston. Experiments were performed using a single production DISI fuel injector within a controlled environment. The controlled environment is contained within a sealed quartz cylinder, which eliminates piston and air motion and allows for independent variation of various experimental parameters such as in-cylinder pressure, piston temperature, and fuel temperature. Axial flow visualization, PIV, and IR imaging experiments were performed for the single injector, with one fuel rail pressure and the simulation of four before top dead center (BTDC) conditions. Two parameters were varied in the experiments: piston surface temperature and fuel temperature with a single boundary condition of piston location (related to in-cylinder pressure through a simple model). It is anticipated that these results will be used within an optical engine to assist in the determination of the optimal injection strategies for reducing fuel impingement on piston surfaces to improve combustion efficiency. These results may also be used to advance injector design to reduce hydrocarbon emissions in DISI engines.

Overall, the use of a simulated piston had very little effect on overall fuel spray structure. The penetration distances and spray cone angles for the piston and no piston

cases are nearly identical for the four BTDC cases. The introduction of the piston caused a 1.8% decrease, 1.1% increase, and a 0.84% decrease in overall penetration distance for the 60° BTDC, 80° BTDC, and 100° BTDC cases, respectively. The introduction of the piston also caused a 2.0% decrease, 4.4% increase, and no change in developed spray angle for the 60° BTDC, 80° BTDC, and 100° BTDC cases, respectively at 1.4 ms after the SOF. Although the use of the simulated piston appears to not alter the spray structure, fuel spray structure is strongly affected by injection timing (and hence, the in-cylinder pressure). In general, the size of the hollow cone decreases as in-cylinder pressure increases. The overall size of the spray becomes increasingly compact as in-cylinder pressure increases. The boundary condition of varying piston location had no effect on fuel spray structure until impact occurs in the piston case. Standard deviation of the penetration distance was found to generally increase as time after the SOF increases.

A statistical analysis was performed on the piston/no piston data in order to better analyze the overall data set. It was concluded that the use of the simulated piston caused no statistical difference in penetration distance of the clump between the two cases (piston and no piston). It was also found that the use of the simulated piston caused no statistical difference in exit spray angle between the two cases (piston and no piston). All three factors (BTDC condition, time after SOF, and the use of the simulated piston condition) had a statistically significant effect on developed spray angle at the 95.0% confidence level.

Fuel spray structure using piston surface and fuel temperature variation is also nearly identical. The overall results reveal nearly identical penetration distances for the ambient and heated fuel cases. The use of higher piston surface temperatures with ambient fuel tended to increase penetration distances while the increase of piston surface temperature using heated fuel (90°C) decreased overall penetration distances. It was also found that as piston surface and fuel temperature increased, developed spray cone angle generally decreased. In 86% of the trials for the 60° BTDC, 80° BTDC, and 100° BTDC cases, developed cone angle decreased as a function of increasing piston surface and fuel temperature. Developed cone angle increases were found at all experimental cases for BDC. Knowledge of the instantaneous DISI fuel spray must be understood for the development of mixture preparation strategy and engine controls.

The fuel spray impingement investigation found that increasing piston surface temperature has a direct effect on piston wetting. The amount of fuel present on the piston surface decreases as piston surface temperature increases. The amount of fuel impinging upon the piston surface increases as time after the SOF increases. A simple technique was developed to better analyze fuel wetting on the piston surface. This technique subtracts the pixel values of one image from another to obtain qualitative data on piston surface wetting. PIV showed that the use of a heated piston had no significant impact on the velocities of the impinging fuel clump for the two times after the SOF used in this work. The clump velocity does appear to be time-dependent, with decreasing clump velocity as time after injection increases (due to increased drag). It was found that

increasing time after the SOF from 1.4 ms to 2 ms decreased velocities (by nearly a factor of three) and reduced overall clump size. A preliminary technique using infrared (IR) imaging revealed a significant change in piston surface temperature with the impact of fuel droplets and wetting of the piston surface is not uniform due to the impinging fuel jet characteristics. Since the most interesting operating mode for DISI engines is late injection, knowledge of the complex interactions involved in piston surface impingement is important in reducing hydrocarbon emissions for future DISI engine design.

Table of Contents

Acknowledgments.....	iv
Executive Summary.....	vi
Table of Contents.....	x
List of Tables	xv
List of Figures	xvii
Chapter 1 Introduction.....	1
1.1 Project Overview	1
1.2 Laboratory Involved.....	4
1.3 Research Motivation	5
1.4 Summary of Results.....	7
1.5 Thesis Outline	9
Chapter 2 Overview of Experimental Techniques.....	10
2.1 Introduction.....	10
2.2 Flow Visualization.....	10
2.2.1 Flow Field Markers.....	11
2.2.2 Flow Visualization Classifications	12
2.2.3 Scattering	15
2.3 Particle Image Velocimetry	18
2.3.1 Interrogation Techniques	20
2.3.2 Digital Particle Image Velocimetry	24

2.4 Nonintrusive Measurement Technique Applications.....	24
2.4.1 Common Flow Visualization Applications.....	25
2.4.2 Common Particle Image Velocimetry Applications	26
2.4.3 Flow Visualization in Sprays	27
2.4.4 Particle Image Velocimetry in Sprays	29
Chapter 3 Literature Survey.....	30
3.1 Introduction.....	30
3.2 DISI Engine Technology	31
3.2.1 Direct Injection Technique	34
3.2.2 Spray Impingement.....	37
3.2.3 Emissions	40
3.3 Sprays.....	43
3.3.1 Fundamental Sprays.....	43
3.3.2 DISI Sprays (Pressure Swirl Injectors).....	46
3.4 Experimental Parameters	49
3.4.1 Piston Temperatures.....	49
3.4.2 Fuel Temperatures	52
Chapter 4 Experimental Setup and Procedures.....	54
4.1 Introduction.....	54
4.2 Experimental Setup.....	54
4.3 In-Cylinder Pressure Control	58

4.4 In-Cylinder Pressure Matching	59
4.5 Fuel Rail Pressure Control	62
4.6 Simulated Piston Design	63
4.6.1 Simulated Piston Components	63
4.6.2 Simulated Piston Temperature Control	65
4.6.3 Final Piston Design	66
4.7 Fuel Rail Temperature Control	67
4.7.1 Fuel Rail Heating System	68
4.8 Laboratory Software and Procedures	70
4.8.1 Flow Visualization and PIV Software	70
4.8.2 Heating System Procedure	73
4.9 Mass Flow Uncertainty	77
Chapter 5 Flow Visualization Results	79
5.1 Introduction	79
5.2 Spray Measurements	81
5.3 Piston and No Piston	83
5.4 Statistical Analysis	92
5.5 Variation of Piston Surface and Fuel Temperature	94
5.6 Summary of Results	101
Chapter 6 Fuel Spray Impingement on Piston Surfaces	128
6.1 Introduction	128

6.2 Piston Surface Impingement	130
6.3 Image Subtraction	133
6.4 Fuel Spray Impingement PIV	134
6.5 Infrared Thermography Flow Visualization	138
6.5.1 IR Setup	139
6.5.2 IR Imaging Approach	140
6.5.3 IR Camera Setup	141
6.5.4 Image Synchronization	142
6.5.5 Technique demonstration.....	144
6.6 Summary of Results.....	145
Chapter 7 Conclusions and Recommendations.....	165
7.1 Conclusions.....	165
7.2 Recommendations.....	170
References.....	172
Appendix A Simulated Piston Designs.....	190
Appendix B Flow Visualization Comparing the Effect of a Simulated Piston on Spray Structure.....	194
Appendix C Flow Visualization Comparing the Effect of a Heated Simulated Piston and Heated Fuel on Spray Structure	222
Appendix D Flow Visualization Comparing the Effect of Piston Surface Temperature on Fuel Spray Impingement.....	295

Appendix E Piston Surface Impingement Image Subtraction	314
Appendix F Penetration Distance Plots Comparing the Effects of Heated Simulated Piston and Heated Fuel	333
Appendix G Statistical Analysis of Penetration Distance, Exit Spray Angle, and Developed Spray Angle Data for the Piston/No Piston Cases.....	340
Curriculum Vitae	384

List of Tables

Table 4-1. Summary of experimental conditions.....	56
Table 4-2. Summary of experimental programs.	71
Table 5-1. Summary of developed and exit spray angles for the piston and no piston cases at 1.4 ms after the SOF.	89
Table 5-2. Summary of developed and exit spray angles for the piston and no piston cases at 2.0 ms after the SOF.	91
Table 5-3. Summary of developed spray angles for piston surface and fuel heating cases.	99
Table G-1. Analysis of Variance for Penetration Distance - Type III Sums of Squares.	342
Table G-2. Least Squares Means for Penetration Distance with 95.0 Percent Confidence Intervals.....	343
Table G-3. Multiple Range Tests for Penetration Distance by BTDC.	345
Table G-4. Multiple Range Tests for PD by Piston/No Piston.	347
Table G-5. Multiple Range Tests for Penetration Distance by Time.	349
Table G-6. Analysis of Variance for Exit Spray Angle - Type III Sums of Squares.....	357
Table G-7. Least Squares Means for Exit Spray Angle with 95.0 Percent Confidence Intervals.....	358
Table G-8. Multiple Range Tests for Exit Spray Angle by BTDC.....	359
Table G-9. Multiple Range Tests for Angle by Time after the SOF.	361

Table G-10. Least Squares Means for Exit Spray Angle with 95.0 Percent Confidence Intervals.....	363
Table G-11. Analysis of Variance for Developed Spray Angle - Type III Sums of Squares.....	366
Table G-12. Least Squares Means for Developed Spray Angle with 95.0 Percent Confidence Intervals.	367
Table G-13. Multiple Range Tests for Developed Spray Angle by BTDC.	368
Table G-14. Multiple Range Tests for Developed Spray Angle by Time after the SOF.	370
Table G-15. Multiple Range Tests for Developed Spray Angle by the Piston/No Piston.	372
Table G-16. Regression Analysis - Linear model: $Y = a + b \cdot X$	374
Table G-17. Analysis of Variance.	374
Table G-18. Analysis of Variance with Lack-of-Fit.....	376
Table G-19. Predicted Values.	377
Table G-20. Comparison of Alternative Models.	378
Table G-21. Unusual Residuals.	379
Table G-22. Influential Points.....	381

List of Figures

Figure 2-1. Stokes and Anti-Stokes Radiation.....	17
Figure 2-2. The fundamental principle of PIV.....	19
Figure 2-3. Interrogation spots in cross-correlation.....	23
Figure 3-1. Configuration of a typical DI engine.	35
Figure 4-1. Experimental Setup	55
Figure 4-2. Experimental injector calibration at various pulsewidth settings.	57
Figure 4-3. Air purge components for regulating and conditioning air. Other air purge components include an air flow meter and exhaust bridge.....	58
Figure 4-4. Graph of in-cylinder pressure versus crank angle.....	61
Figure 4-5. Fuel supply system, including nitrogen cylinder and fuel bomb.	62
Figure 4-6. Unassembled piston simulator.	64
Figure 4-7. Fuel rail heating system.	69
Figure 4-8. Series 96 inputs and outputs [Watlow Controls (1997), referenced with permission].....	73
Figure 4-9. Series 96 keys and displays [Watlow Controls (1997), referenced with permission].....	74
Figure 4-10. Series 96 navigation [Watlow Controls (1997), referenced with permission].	75
Figure 5-1. Definition of spray parameters for spray cone angle and penetration distance.	81

Figure 5-2. Flow visualization showing instantaneous spray structure with and without the simulated piston. Images taken for the 60° BTDC case, with delay after the SOF shown on the left side of the images. (As shown in Appendix B, using 50 μ s resolution, the clump and cone impact the piston surface at ~0.9 ms and ~1.5 ms after the SOF.)..... 105

Figure 5-2 (con't). Flow visualization showing instantaneous spray structure with and without the simulated piston. Images taken for the 60° BTDC case, with delay after the SOF shown on the left side of the images. (As shown in Appendix B, using 50 μ s resolution, the clump and cone impact the piston surface at ~0.9 ms and ~1.5 ms after the SOF.)..... 106

Figure 5-3. Flow visualization showing instantaneous spray structure with and without the simulated piston. Images taken for the 80° BTDC case, with delay after the SOF shown on the left side of the images. (As shown in Appendix B, using 50 μ s resolution, the clump and cone impact the piston surface at 1.15 ms and 2.45 ms after the SOF.)..... 107

Figure 5-3 (con't). Flow visualization showing instantaneous spray structure with and without the simulated piston. Images taken for the 80° BTDC case, with delay after the SOF shown on the left side of the images. (As shown in Appendix B, using 50 μ s resolution, the clump and cone impact the piston surface at 1.15 ms and 2.45 ms after the SOF.)..... 108

Figure 5-4. Flow visualization showing instantaneous spray structure with and without the simulated piston. Images taken for the 100° BTDC case, with delay after the SOF shown on the left side of the images. (As shown in Appendix B, using 50 μ s resolution, the clump and cone impact the piston surface at 1.85 ms and 3.85 ms after the SOF.).....	109
Figure 5-4 (con't). Flow visualization showing instantaneous spray structure with and without the simulated piston. Images taken for the 100° BTDC case, with delay after the SOF shown on the left side of the images. (As shown in Appendix B, using 50 μ s resolution, the clump and cone impact the piston surface at 1.85 ms and 3.85 ms after the SOF.).....	110
Figure 5-5. Fuel spray penetration showing the effect of the use of a simulated piston as a function of time after the SOF for the 60° BTDC. Penetration calculated as leading edge of clump and determined every 50 μ s from SOF using the average from 10 sets of images.....	111
Figure 5-6. Standard deviation of the penetration distance with and without the simulated piston as a function of time after the SOF for the 60° BTDC case.....	111
Figure 5-7. Fuel spray penetration showing the effect of the use of a simulated piston as a function of time after the SOF for the 80° BTDC. Penetration calculated as leading edge of clump and determined every 50 μ s from SOF using the average from 10 sets of images.....	112

Figure 5-8. Standard deviation of the penetration distance with and without the simulated piston as a function of time after the SOF for the 80° BTDC case.....	112
Figure 5-9. Fuel spray penetration showing the effect of the use of a simulated piston as a function of time after the SOF for the 100° BTDC. Penetration calculated as leading edge of clump and determined every 50 μ s from SOF using the average from 10 sets of images.....	113
Figure 5-10. Standard deviation of the penetration distance with and without the simulated piston as a function of time after the SOF for the 100° BTDC case.	113
Figure 5-11. Flow visualization showing the effect of piston surface and fuel temperature variation on the instantaneous spray structure. Images taken for the 60° BTDC case, with delay after the SOF shown on the left side of the images.....	114
Figure 5-12. Flow visualization showing the effect of piston surface and fuel temperature variation on the instantaneous spray structure. Images taken for the 80° BTDC case, with delay after the SOF shown on the left side of the images.....	117
Figure 5-13. Flow visualization showing the effect of piston surface and fuel temperature variation on the instantaneous spray structure. Images taken for the 100° BTDC case, with delay after the SOF shown on the left side of the images.....	120
Figure 5-14. Flow visualization showing the effect of piston surface and fuel temperature variation on the instantaneous spray structure. Images taken for the BDC case, with delay after the SOF shown on the left side of the images.....	123

Figure 5-15. Fuel spray penetration showing the effect of heated and ambient fuel with a 100°C piston surface temperature for the 80° BTDC. Penetration calculated as leading edge of clump and determined every 50 μ s from SOF using 1 set of images.	126
Figure 5-16. Fuel spray penetration showing the effect of heated and ambient fuel with a 200°C piston surface temperature for the 80° BTDC. Penetration calculated as leading edge of clump and determined every 50 μ s from SOF using 1 set of images.	126
Figure 5-17. Fuel spray penetration showing the effect of piston surface temperature variation with ambient fuel for the 80° BTDC. Penetration calculated as leading edge of clump and determined every 50 μ s from SOF using 1 set of images.	127
Figure 5-18. Fuel spray penetration showing the effect of piston surface temperature variation with hot fuel for the 80° BTDC. Penetration calculated as leading edge of clump and determined every 50 μ s from SOF using 1 set of images.	127
Figure 6-1. Fuel spray impingement using piston surface temperatures of 100°C, 125°C, 150°C, and 175°C, with delay after the SOF shown on the left side of the images. The first column from the left shows full field flow visualization of the spray while all other columns show fuel spray impingement at the given temperatures.	150
Figure 6-2. Image subtractions for the 175°C-100°C showing the effect of pixel range value variation. Full field and piston surface impingement images are provided in	